PCCP

Accepted Manuscript

This is an *Accepted Manuscript*, which has been through the Royal Society of Chemistry peer review process and has been accepted for publication.

Accepted Manuscripts are published online shortly after acceptance, before technical editing, formatting and proof reading. Using this free service, authors can make their results available to the community, in citable form, before we publish the edited article. We will replace this *Accepted Manuscript* with the edited and formatted *Advance Article* as soon as it is available.

You can find more information about *Accepted Manuscripts* in the Information for Authors.

Please note that technical editing may introduce minor changes to the text and/or graphics, which may alter content. The journal's standard Terms & Conditions and the Ethical guidelines still apply. In no event shall the Royal Society of Chemistry be held responsible for any errors or omissions in this *Accepted Manuscript* or any consequences arising from the use of any information it contains.

ROYAL SOCIETY OF CHEMISTRY

www.rsc.org/pccp

TOC for

3D Visualization of Inhomogeneous Multi-Layered Structure and Young's Modulus of Solid Electrolyte Interphase on Silicon Anode for Lithium ion Batteries

Jieyun Zheng,[a] Hao Zheng,[a] Rui Wang,[c] Liubin Ben,[a] Wei Lu,[b] Liwei Chen,[b] Liquan Chen[a] and Hong Li[a*]

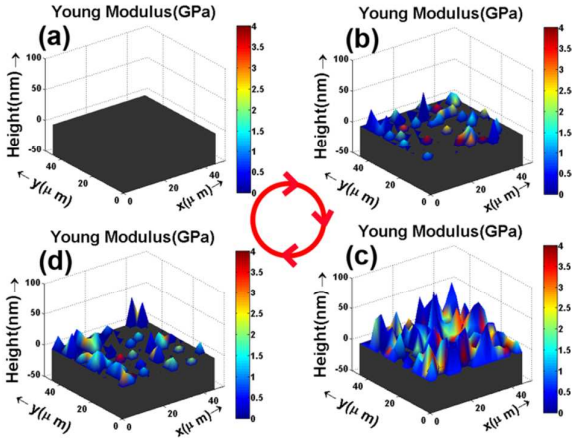

Inhomogeneous multiple-layered structure, thickness, Young's modulus and coverage of SEI on silicon anode during cycling are visualized three-dimensionally by scanning force curve method.

Physical Chemistry Chemical Physics Accepted Manuscript

Journal Name

RSCPublishing

paper

3D Visualization of Inhomogeneous Multi-Layered Structure and Young's Modulus of Solid Electrolyte Interphase (SEI) on Silicon Anode for Lithium ion Batteries

Cite this: DOI: 10.1039/xoxxoooooox

Received ooth January 2012,
Accepted ooth January 2012

DOI: 10.1039/xoxxoooooox

www.rsc.org/

Jieyun Zheng,[a] Hao Zheng,[a] Rui Wang,[c] Liubin Ben,[a] Wei Lu,[b] Liwei Chen,[b] Liquan Chen[a] and Hong Li[a*]

Microstructure and mechanical properties of the solid electrolyte interphase (SEI) in non-aqueous lithium ion batteries are key issues for understanding and optimizing the electrochemical performance of lithium batteries. In this report, the three-dimensionally (3D) multi-layered structures and the mechanical properties of the SEI formed on silicon anode material for next generation of lithium ion batteries have been visualized directly for the first time, through a scanning force spectroscopy method. The coverage of the SEI on silicon anode is also obtained through 2D projection plots. The effects of temperature and the function of additives in electrolyte on the SEI can be understood accordingly. A modified model about dynamic evolution of the SEI on the silicon anode material is also purposed, which aims to explain why the SEI is very thick and how the multi-layered structure is formed and decomposed dynamically.

1. Introduction

Applications of non-aqueous lithium ion batteries are extending rapidly from electronic devices to electric vehicles, renewable energy and many new markets.[1-6] The lithium ion batteries exhibiting high energy density, power density, coulombic efficiency, good cyclability, excellent safety, low polarization and low self-discharge are desirable for practical applications. It is well known that these performances are strongly affected by the features of solid electrolyte interphase (SEI) grown on cathode and anode.[7] A stable SEI with full surface coverage over the electrode is favourable for achieving excellent electrochemical performances of lithium ion batteries.

Understanding SEI is quite challengeable due to its complicated and amorphous structure. The SEI model has been proposed over 30 years. Pioneering investigations on SEI utilizing various techniques[8-13] have shown that the SEI consists of two layers, i. e., an inorganic inner layer close to the electrode surface, which is composed of LiF, Li_2O, Li_2CO_3, et al., and a covering layer which is made up of organic products, e. g., $LiCH_3$, $LiOCO_2CH_3$ and ROLi (R is an organic group dependent on the solvent).[14, 15] These results are quite helpful for understanding the electrochemical reactions for forming the SEI. However, the exact microstructure and mechanical properties of the SEI, in addition to the coverage of the SEI on electrodes are still not very clear. In addition, the coverage of the SEI on electrodes has not been reported. These aspects are critical for understanding the effects of the SEI on the electrochemical performances of the electrodes and batteries. Actually, in spite of wide applications of Li-ion batteries, the SEI still remains arguably "the most important but the least understood aspect in rechargeable Li batteries".[16]

Silicon owns the high specific capacity of 3579 $mAhg^{-1}$ at room temperature for the stoichiometry of $Li_{15}Si_4$. It has been regarded as the most promising anode for the third generation Li-ion batteries.[17-19] However, unstable SEI and large volume change result in poor cycling stability in full cells.[20, 21] It is known that large volume variation may cause mechanical breakdown of the brittle silicon material, leading to exposure of fresh silicon surface to the electrolyte. This could trigger the further growth of the fresh SEI and consequently causes capacity loss. Achieving high coulumbic efficiency (> 99.9%) in successive cycles is still difficult but very important for practical application of silicon anodes. In order to approach the target, besides the optimization of the microstructure and composition of the Si-based materials, it is also essential to understand the surface properties of the SEI on Si as well as the function of SEI film formation additive in electrolyte.

In this work, the multi-layered structure and mechanical properties of the SEI formed on the silicon anode material in lithium ion batteries have been visualized three-dimensionally (3D) for the first time, through a scanning force curve method using scanning probe microscope. The coexistence of single-layered, double-layered and multi-layered structures with varied Young's modulus as well as the thickness distribution on the surface of silicon anode has been observed. The effects of elevated temperature (55°C) and the SEI additive, vinylene carbonate (VC), are also investigated. A novel mechanism of

Physical Chemistry Chemical Physics Accepted Manuscript

the dynamic evolution of the SEI on the silicon anode material is proposed accordingly, which could explain why the SEI is very thick and how the multi-layered structure is formed.

2. Experimental section

Dozens of silicon thin film electrodes were prepared under the same condition by a magnetron sputtering method: Ti was deposited on polished quartz substrate by DC magnetron sputtering as current collector. Then silicon was deposited on Ti directly by RF magnetron sputtering. The chamber reached 2×10^{-4} Pa before sputtering and kept at 0.5 Pa under high purity Ar (99.999%) during sputtering. A Swageloke-type two-electrode cell was assembled in an Ar-filled glove box, silicon thin film electrode was used as the working electrode and lithium foil as the counter electrode. The electrolytes were 1 mol·L^{-1} $LiPF_6$ dissolved in ethylene carbonate (EC): dimethyl carbonate (DMC) (1:1) with or without 2 wt. % VC. Electrochemical cycles were carried out using an ARBIN automatic battery tester between 2V and 0.005V. After cycling, the cells were disassembled in an Ar-filled glove box and the silicon thin film electrodes were washed by anhydrous DMC to make sure no residual of $LiPF_6$. Then the samples were dried in the vacuum chamber for more than 5 hours before further measurement. All the samples were transferred to a MultiMode 8 (BRUKER) scanning probe microscopy (SPM) equipped in an Ar-filled glove box. Peakforce tapping mode was chosen for topographic imaging process. In order to draw a 3D plot, 225 forces curves were recorded in a 45 × 45 μm^2 square region with the uniform positional distribution, the thickness and Young's modulus were read out from each force curve. Thus the coordinates of each layer of SEI is (X, Y, Z), X=0, 3, 6…, Y=0, 3, 6…, Z axis is represented by the thickness of SEI. Young's modulus was delivered by the color bar.

3. Results and discussion

3.1 Morphology and roughness variation of silicon anode

SEM image, XRD pattern and Raman spectra of the as-prepared silicon thin film electrode are shown in Figure 1. It can be seen that the as-deposited thin film is flat, dense and the thickness is about 450 nm. The broad diffraction pattern around 22° is from quartz substrate, as shown in Figure 1b, other peaks in the pattern could be related to the Ti_xSi_y alloy (Ti_3Si_5, $TiSi_2$), and no crystalline silicon peak is found in the diffraction pattern. From the Raman spectra (Figure 1c), the peak around 472 cm^{-1} can be observed clearly as the characteristic of amorphous silicon. Accordingly, the obtained thin film is amorphous silicon film, with impurity phase at the interface region between Ti layer and silicon layer.

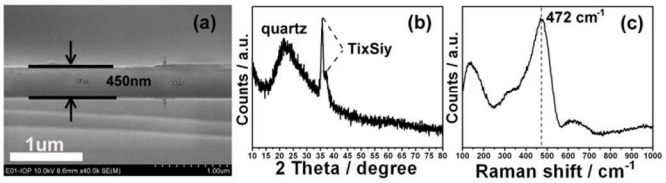

Fig. 1 (a) SEM cross section image, (b) XRD pattern, (c) Raman spectra of silicon thin film electrode.

The electrodes were discharged and charged to different states and named as the Samples 1-18 as listed in Table 1. Figure 2 and Figure S1 indicate corresponding voltage profiles of each sample. The Sample 1 is the pristine silicon electrode without electrochemical test. The lithiation behaviors showed in Figure S1 and Figure 2a of the amorphous silicon anodes are identical as previous reports.[20, 22]

Sample Number	Electrochemical states	Electrolyte & temperature
Sample 1	Pristine silicon	VC free RT
Sample 2	Discharge to 0.2V	
Sample 3	Discharge to 0.05V	
Sample 4	Discharge to 0.005V	
Sample 5	Charge to 0.6V, relative to Sample 4	
Sample 6	Charge to 2V,	
Sample 7	Discharge to 0.005V and keep at 0.005V for 48h,	
Sample 8	Charge to 0.6V, relative to Sample 7	
Sample 9	Charge to 1V	
Sample 10	Charge to 2V	
Sample 11	Discharge to 0.005V and keep at 0.005V for 48h	VC free 55°C
Sample 12	Charge to 0.6V relative to Sample 11	VC free RT
Sample 13	Charge to 1V	
Sample 14	Charge to 2V,	
Sample 15	Discharge to 0.005V and keep at 0.005V for 48h	2 wt.% VC RT
Sample 16	Charge to 0.6V, relative to Sample 15	
Sample 17	Charge to 1V	
Sample 18	Charge to 2V	

Table 1 Silicon thin films at different electrochemical states for force curve testing.

Surface morphology evolution of the silicon anode was detected, as shown in Figure 2c-h. The morphology of surfaces (3×3 μm^2) at different stages and their differences can be easily distinguished from the height profiles. Pristine silicon anode exhibits spherical grain surface, and the grain size ranges from tens to hundreds of nanometers. In order to indicate the surface morphology change quantitatively, the roughness (R_q) analysis is performed. R_q can be expressed as equation (1):

$$R_q = \sqrt{\frac{\sum_i^N (Z_i - \bar{Z})^2}{N}} \quad (1)$$

Where Z_i is the height value of the AFM topography image, $\bar{Z}$ is the mean value of the height data, N is the number of points within the image.

The roughness can be measured by root-mean-squared (RMS) values determined from the AFM images as we can see from Figure 2b that the electrode surface roughness increases gradually. This phenomenon is also observed on other anode materials of lithium ion batteries.[23-26] After discharging to 0.005V, the surface became somewhat blurred. In the charging process, cracks appeared in the anode labeled by the yellow dash lines as shown in Figure 2g and 2h. After charging to 2V, the spherical grain appeared on the pristine silicon anode was hardly discernable. The roughness (Figure 2h) at 2V is even less than of that of original anode, this may be caused by two factors. One lies in the volumetric shrinkage after charging process, which could lead to the reduced size of surface particle, as can be seen in Figure 2h, the other reason is that the SEI may

Physical Chemistry Chemical Physics Accepted Manuscript

 This journal is © The Royal Society of Chemistry 2012

deposit on the "valley" space among the grains, the existence of SEI in the charging state will be confirmed later in this article. And this can also make the surface smoother.

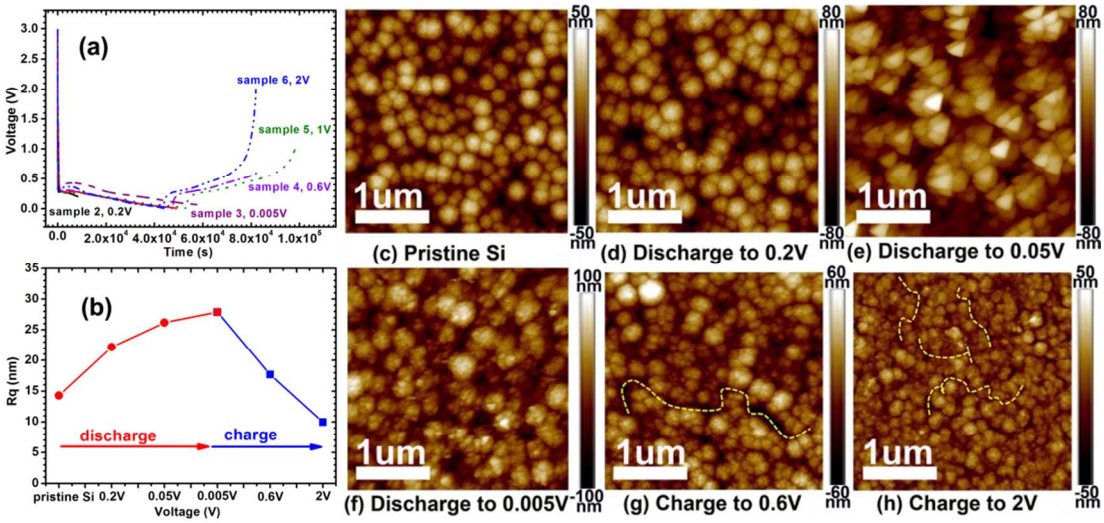

Fig. 2 (a) Voltage profiles of sample 2-6, which were discharged to 0.2, 0.05, and 0.005V, charged to 0.6, and 2V, respectively. (b) Surface roughness of the sample above. (c) - (h) AFM topographical images ($3 \times 3\mu m^2$) of sample 1-6, where sample 1 was pristine silicon thin film.

3.2 Force curves of discharged silicon anode

Principle of the force curve method for detecting the SEI has been introduced in our previous report.[26] The representative force curves and purposed possible corresponding structures of the SEI films on the silicon anode are illustrated in Figure 3. In general, there are seven types of representative force curves. According to the features of the force curves, we could suggest possible micro-structure of the complicated surface film on lithiated silicon electrodes.

The first type of the surface structure is the naked surface. The corresponding force curve is shown in Figure 3a. In this figure, three types of force curve are compared. The black solid line is the typical mechanical response of uncycled silicon anode. The force increases sharply even the indentation depth is very small, indicating the surface is very hard. The red dash line is the typical response of the naked surface on the lithiated silicon anode after cycling. It is also a linear response but the slope is lower than that for the naked one. This is reasonable since it is already known that the amorphous Li-Si alloy samples formed during cycling becomes softer than initial amorphous silicon according to theoretical calculation of Young's modulus.[27] The blue dot line in Figure 3a exhibits an initial moderate rising, followed by a flat increase then a sharp one. The former is perceived as the mechanical response of the relatively soft SEI and the latter is the response of the formed Li-Si alloy beneath the SEI film since the slope is comparable to the cycled silicon electrode. This curve is shown clearly in Figure 3c. In this figure, the indentation depth $\delta = 0$ nm is the starting-contact point of the tip on the surface, a set of elastic ($0<\delta<20$nm, a linear slope in the indentation curve) and plastic yield ($20<\delta<52$ nm, the slope decreased compared with the elastic region) region exist in the force curve. We could draw a conclusion safely from such a response that the detected area with the response as Figure 3c is covered by a single layer SEI film.

Another type of the force curve is exhibited as shown in Figure 3e. The enlarged force curve is shown again in Figure S2a and S2b. A set of elastic and yield region is seen from 18 nm-70 nm, another set is 0-18 nm, which can be clearly observed in Figure S2b. Compared to Figure 3c, we propose that this area could be covered by a double-layered structure as shown in Figure 3f, which has varied mechanical responses at different depth but the same surface position.

Similarly, triple-layered structure can be also seen in the surface as shown in Figure 3 g-h. Each layer is identified by one set of elastic and yield region. There are three sets of such responses at different depth and the same surface position.

In some cases, the force curve jumps to a certain value then shows the single layer or double layer responses as mentioned above. This could be caused by the existence of a hard tiny particle floated on the surface. The tip touches the hard particle firstly, and the tip can push the particle downward when higher force is applied. Such response can be seen in Figure 3i and 3j.

Similar to the case in Figure 3i, it is also reasonable that the hard tiny particle stays in the interior position sandwiched by two top and bottom soft layers. We presume that the responses in the Figure 3k could be caused by the structure shown in Figure 3l.

Some curves show that the force increases gradually after increasing the indentation length, but drops down when the indentation length of the tip increase further and then increase again, as shown in Figure 3m. the enlarged force curves are shown in Figure S2c and S2d. The drop down of the force curve could mean that the place touched by the tip is empty at certain place. It has been suggested that the micro-pore or meso-pore could remain in the SEI due to the release of the gas during the formation of the SEI film.[28] It is quite possible that the curves shown in Figure 3m is related to the microstructure shown in Figure 3n in which a bubble is remained in the SEI film.

Physical Chemistry Chemical Physics Accepted Manuscript

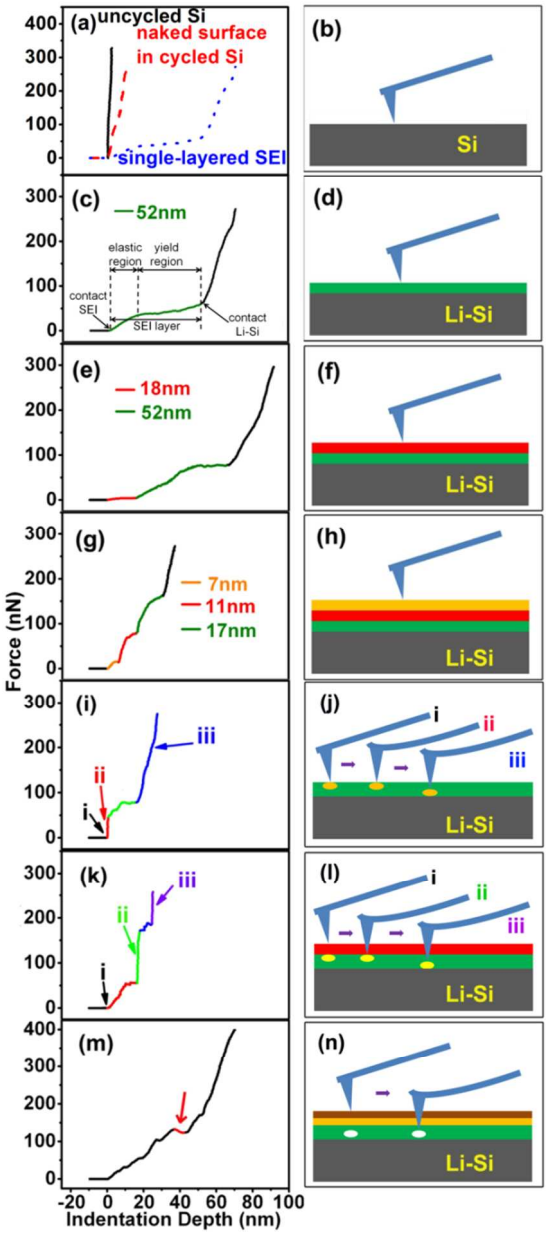

Fig. 3 Layered structure of SEI. Typical profiles of force curve spectroscopy: (a) mechanical response of the uncycled silicon, naked surface in cycled silicon and SEI, (c) (e) (g) are single-layered, double-layered and triple-layered, (i) hard particle, (k) hard particle sandwiched by two soft layers, (m) bubble, (b), (d), (f), (h), (j), (l), (n) are the possible models for the previous structures, respectively.

3.3 Thickness statistics of the SEI on discharged silicon electrode

According to above analysis, it is easily to judge whether the surface area of discharged silicon electrodes is covered by the SEI or not based on the mechanical responses of the force curves. From the force curve, the thickness of each layer of SEI can be also obtained since the depth that the tip touches the lithiated silicon electrode substrate can be known as mentioned above. Figure 4 indicates the total thickness of the SEI film at a certain place on the silicon electrodes in two electrolytes with and without VC additive. In order to see the difference easily, three different reaction routes are directed by the arrows with different colors. It can be found from Figure 4 that the SEI grows thicker upon the discharging process (lithiation) and the thickness is reduced during charging. This indicates clearly that the SEI on silicon electrode is not as stable as that on graphite anode.

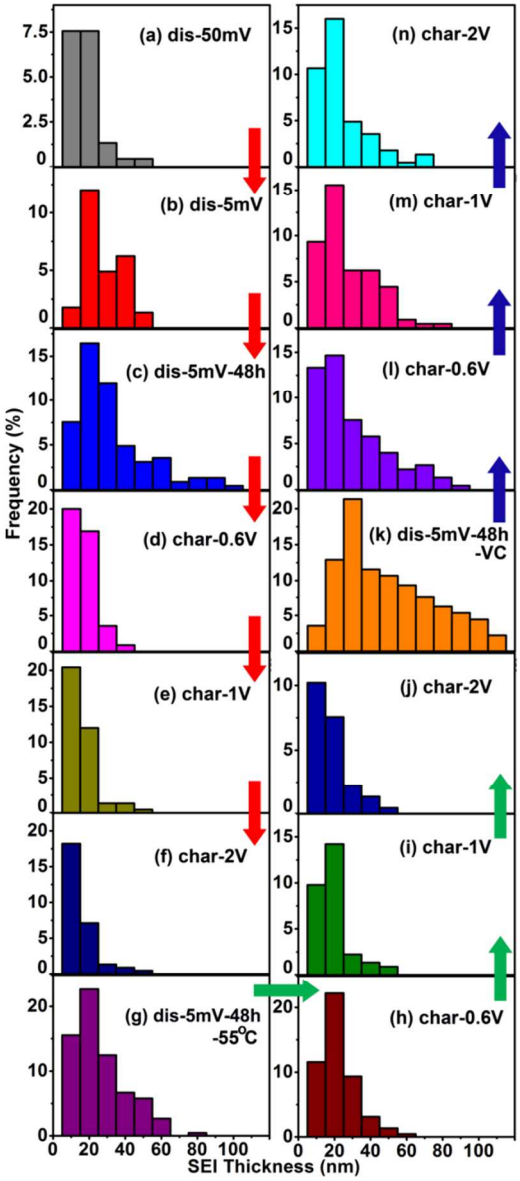

Fig. 4 Thickness distribution. (a)-(n) thickness of SEI for sample 3, 4 (discharge to 0.05,0.005V, RT, VC free), sample 7 (discharge to 0.005V and keep at 0.005V for 48h, RT, VC free), sample 8-10(charge to 0.6V, 1V, 2V, RT, VC free), sample 11(discharge to 0.005V and keep at 0.005V for 48h, 55°C, VC free), sample 12-14 (charge to 0.6V, 1V, 2V, RT, VC free), sample 15 (discharge to 0.005V and keep at 0.005V for 48h, RT, 2wt.% VC), sample 16-18 (charge to 0.6V, 1V, 2V, RT, 2wt.% VC)

In addition, we supposed that the SEI should grow thicker at 55°C compared to the room temperature. Surprisingly, the SEI on fully discharged silicon electrode at 55°C has less amount of the thick SEI (> 60 nm) than that discharged at room temperature. Accordingly, it seems that the thicker SEI part tends to dissolve in the electrolyte. This is reasonable if the

Physical Chemistry Chemical Physics Accepted Manuscript

This journal is © The Royal Society of Chemistry 2012

thicker part is composed of polymer-like or organic SEI species with relatively high solubility at elevated temperature. It can be also found from Figure 4c and 4k that the addition of VC is favorable for forming thicker SEI and the thickness distribution of the SEI is more continuously compared to VC-free electrolyte. Compared Figure 4n with Figure 4f and Figure 4j, the population of the remained SEI in VC-added electrolyte is higher than VC free electrolyte both at room temperature and 55°C. These results mean that VC is very helpful to form more stable SEI film on the silicon electrode.

3.4 Young's Modulus of the SEI film

Young's modulus regarding the SEI can be extracted from the force curves. The interaction between the tip and sample is described as penetration of a conical tip (tip radius~2nm) into the flat surface. The relationship among the Young's modulus, loading force, indentation depth can be expressed with the Sneddon model.[26, 29]

$$F = (2/\pi)\,(E/(1-\nu^2))\,\delta^2 \tan(\alpha) \quad (2)$$

F is the applied force, δ is the indentation of elastic region, E is the Young's modulus, α= 20° is the half cone angle of the AFM probe, and ν is the Poisson ratio, which is set to be 0.5, assuming rubber elasticity for SEI films at the early stage of elastic region.[26]

Thickness and Young's modulus of each layer of the SEI at a certain place formed at different states are shown in Figure 5, 6, 7. The layered feature of the SEI is marked using different color. Figure 5 a-f shows the Thickness vs. Young's modulus of the sample 3, 4, sample 7-10. The Sample 2 discharged to 0.2 V was not shown here since there is no SEI on the surface being identified. It is found that the SEI formed at 0.05 V is single-layered structure with a thickness less than 40 nm. And the thicker area shows lower Young's modulus. Double-layered SEI can be observed in the state of discharged to 0.005 V as shown in Figure 5b and the multi-layered SEI appears in the state that the silicon electrode was discharged to 0.005 V then kept at 0.005V for 48 hours (Figure 5c). It is obviously that the SEI grows thicker during discharging and more SEI species with lower Young's modulus appear at fully discharged state. During charging, the SEI areas with multi-layered structure decreases as shown in Figure 5d-e. After charging to 2.0 V as shown in Figure 5f, only single–layer structured SEI remain. This indicates clearly that the multi-layer structured SEI is formed gradually and the softer SEI areas can be decomposed during the charging. It is known that organic and polymer-like SEI on the surface of Cr_2O_3 anode is decomposed gradually during charging, as evidenced by TG-DSC-MS experiment.[30] The electrochemical instability SEI on silicon anode shown in Figure 5 is consistent with our previous investigation on Cr_2O_3 anode. It should be mentioned here that the existence of SEI in the charging state is confirmed in Figure 5f, therefore, the roughness of the silicon surface at the charged state will be influenced by the SEI, as shown in Figure 2f.

Figure 6 indicates the effect of the temperature. It can be seen in Figure 6a that the soft SEI parts on fully discharged silicon anode are much less than that at room temperature. The electrochemical decomposition reactions of the electrolyte should be accelerated at 55°C compared to the electrode at room temperature. Therefore, this result means that the soft SEI at 55°C is dissolved. The hard part, which should be composed of inorganic species, is remained at 55°C. Figure 6b-e consist with the results shown in Figure 5c-f, the soft SEI parts are electrochemically decomposable.

The effect of the addition of VC in the electrolyte is also investigated. VC is famous to improve the cyclic performance of silicon anode.[25, 31] It has been suggested that the addition of VC should be helpful to form "better" SEI film to protect lithiated silicon anode. However, up to now the details of the SEI after adding VC is not clear. As shown in Figure 7a, the population of the SEI is much higher than that without VC additive. Compared Figure 7e with Figure 5f, it is obviously that more SEI areas remain after adding VC. This does confirm the effect of the VC. Such evidence is not available before.

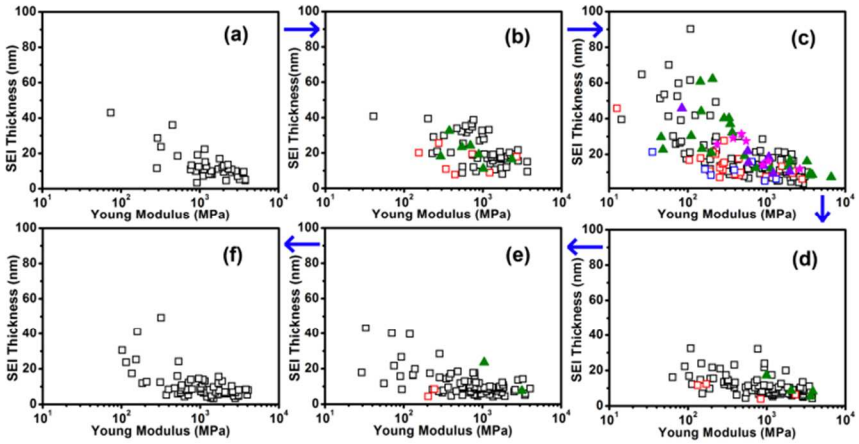

Fig. 5 Relation between SEI thickness and Young Modulus for samples 3 (a, discharge to 0.05V, RT, VC free), 4 (b, discharge to 0.005, RT, VC free), 7 (c, discharge to 0.005V and keep at 0.005V for 48h, RT, VC free**),** Sample 8-10 (d-f, charge to 0.6V, 1V, 2V, RT, VC free). Black square "□" are for single-layered SEI films; red square "□" are for outer layer, olive triangle "▲" are for inner layer of double-layered SEI films; blue square "□" are for outer layer, violet triangle "▲" are for middle layer, magenta pentagon "★" are for inner layer of triple-layered SEI films.

Physical Chemistry Chemical Physics Accepted Manuscript

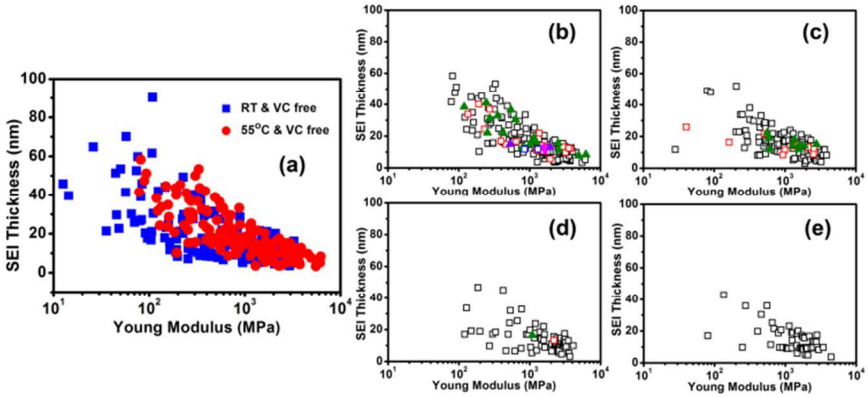

Fig. 6 (a) Comparison of Sample 7 and 11, (b)-(e) Relation between SEI thickness and Young Modulus for samples 11 (discharge to 0.005V and keep at 0.005V for 48h, 55°C, VC free), 12-14 (charge to 0.6V, 1V, 2V, RT free). Black square "□" are for single-layered SEI films, red square "□" are for outer layer, olive triangle "▲" are for inner layer of double-layered SEI films; blue square "□" are for outer layer, violet triangle "▲" are for middle layer, magenta pentagon "★" are for inner layer of triple-layered SEI films.

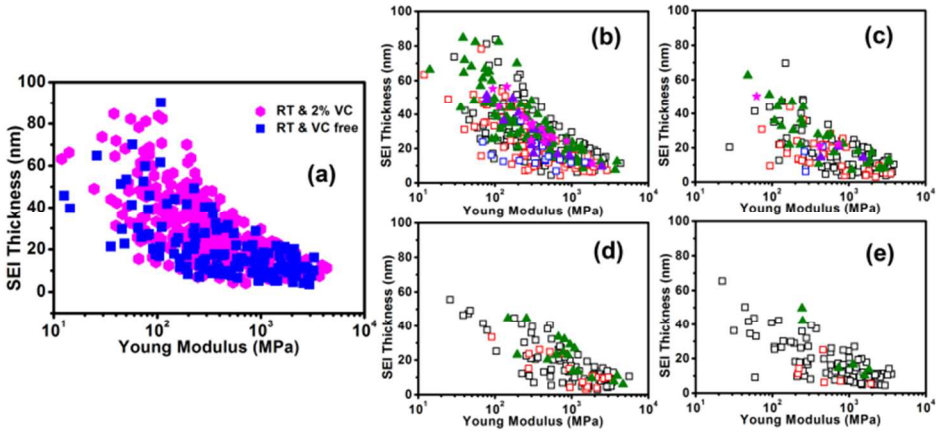

Fig. 7 (a) Comparison of Sample 11 and 15, (b)-(e) Relation between SEI thickness and Young Modulus for samples 15 (discharge to 0.005V and keep at 0.005V for 48h, RT, 2% VC), 16-18 (charge to 0.6V, 1V, 2V, RT, 2% VC). Black square "□" are for single-layered SEI films, red square "□" are for outer layer, olive triangle "▲" are for inner layer of double-layered SEI films; blue square "□" are for outer layer, violet triangle "▲" are for middle layer, magenta pentagon "★" are for inner layer of triple-layered SEI films.

3.5 3D Young's modulus plot of discharged silicon anode

Since the Young's modulus at each position at different indentation length on the surface of discharged silicon anode are known, a 3D Young's modulus plot of discharged silicon electrode after analyzing all force curves in a certain area can be drawn. Figure 8 shows such 3D plot of the SEI on silicon anode at different states, the three different reaction routes are directed by the arrows with different colors, same as Figure 4. The letter a, b, c… at the top left corner of the figures is corresponding to the different electrochemical states also labeled by the same letters (a, b, c…) in the voltage profiles. It can be seen clearly that the silicon anode is covered by SEI inhomogeneously, as wild forest. Some areas are not covered and some areas are covered by thicker SEI. The soft part SEI is always covering on the outer layer. This can be also obtained from a cross-section view of 3D plot, as shown in Figure 9. Uncovered area, the area with different layered structure with different Young's modulus can be observed clearly.

By comparing the SEI grown under three reaction routes, it can be seen that VC (arrow with blue color) is effective to form much more stable SEI.

Physical Chemistry Chemical Physics Accepted Manuscript

 This journal is © The Royal Society of Chemistry 2012

Journal Name RSCPublishing

paper

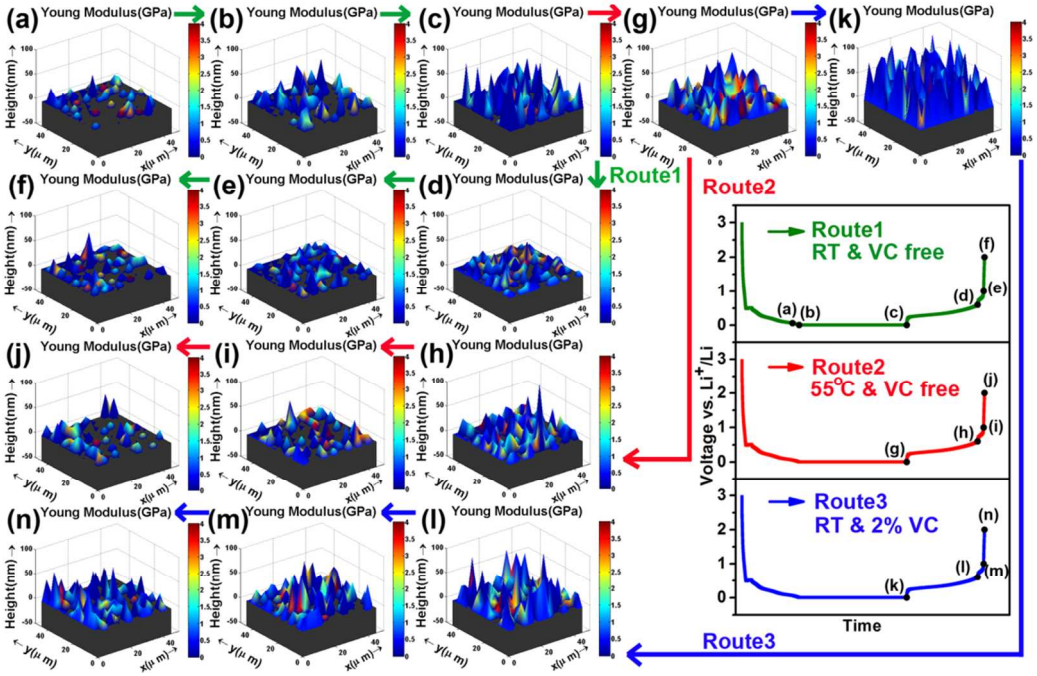

Fig. 8 Three-dimensional plots for sample 3, 4(a-b, discharge to 0.05V, 0.005V, RT, VC free), Sample 7(c, discharge to 0.005V and keep at 0.005V for 48h, VC free, RT), Sample 8-10 (d-f, charge to 0.6V, 1V, 2V, RT, VC free), Sample 11 (g, discharge to 0.005V and keep at 0.005V for 48h, 55°C, VC free), Sample 12-14 (h-j, charge to 0.6V, 1V, 2V, RT, VC free), Sample 15 (k, discharge to 0.005V and keep at 0.005V for 48h, RT, 2wt.%VC), Sample 16-18 (l-n, charge to 0.6V, 1V, 2V, RT, 2wt.%VC). Black substrates are for Li-Si alloy at different states, x, y axis is for coordinates, z axis is for thickness of SEI films. The color bar of 0-4GPa is the Young Modulus for the SEI films.

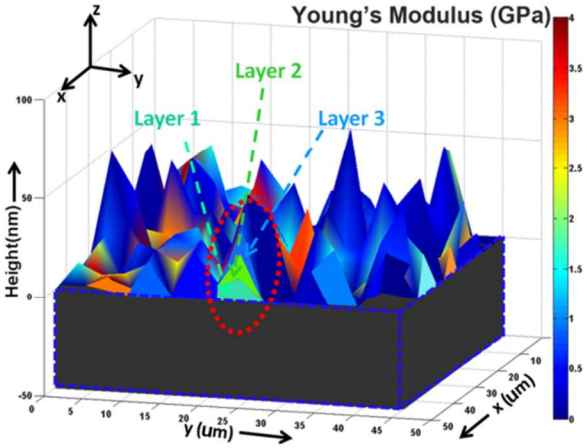

Fig. 9 Cross section view of 3D plots.

3.6 SEI coverage on discharged silicon electrode

In literature, it is always presumed that the SEI will cover on the surface of the anode completely since the electrolyte should obtain electrons from exposed area, reduced locally and formed SEI will grow on the exposed area spontaneously. Many reported TEM images on single or a few particles seem support this viewpoint. However, there is no reliable data to provide the SEI coverage information. Actually, if above suggestion is correct, the coulombic efficiency of the anodes in the successive cycles should be closed to 100% if the SEI can cover the surface of the anode completely after the first discharging.

Since we already obtain the 3D SEI plot, 2D projection of 3D plots can be visualized, as shown in Figure 10. It is quite clear that the SEI does not cover the whole surface in each state. It looks like that the highest coverage of the SEI on silicon anode is Figure 10k, corresponding to the fully discharged silicon anode with VC additive.

The coverage of the SEI film can be calculated quantitatively as equation (3):

coverage = Number (SEI response)/Total number of force curve (3)

As shown in Figure 11, the coverage of the SEI continually increases in the discharging process. Without VC additive, the SEI coverage on the fully discharged silicon anode is only 51.6% at room temperature. This value increases to 66.2% for the silicon anode discharged at 55°C, although the soft parts seem dissolved in the electrolyte, as mentioned above. While the SEI coverage of the discharged silicon anode after adding 2 wt. % of VC increases to 95.1%. This result could explain why adding

Physical Chemistry Chemical Physics Accepted Manuscript

VC is very effective for silicon anode, as confirmed by the electrochemical tests previously.

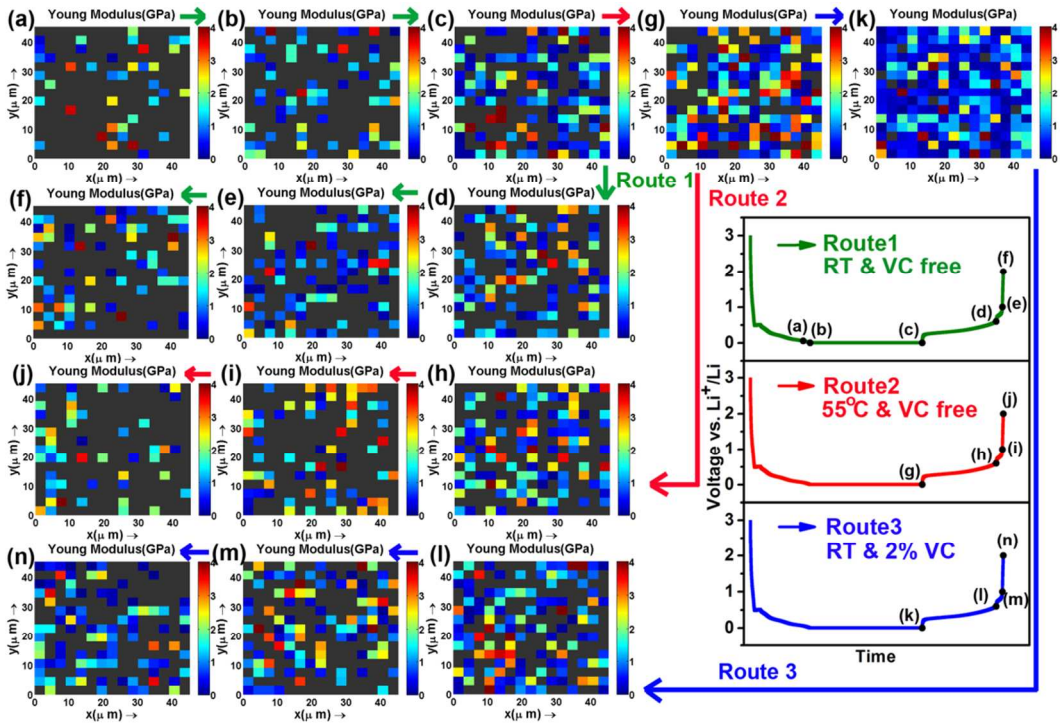

Fig. 10 3D projection of 3D plots in Figure 8

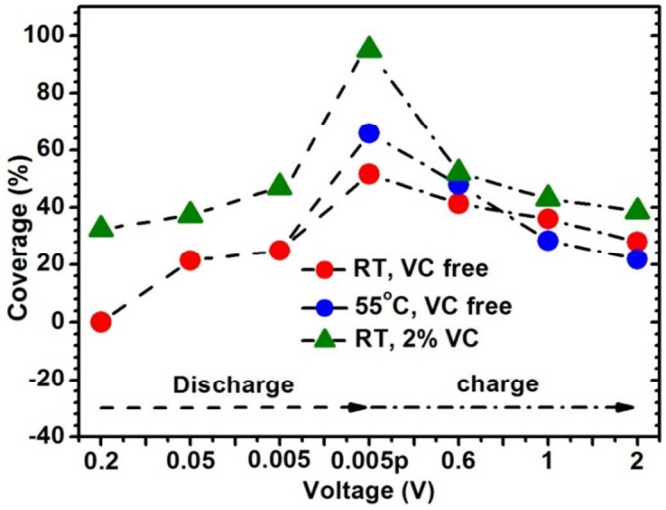

Fig. 11 Statistics of coverage. SEI coverage of the sample 2-4 (discharge to 0.2V, 0.05V, 0.005V, RT, VC free), Sample 7 (discharge to 0.005V and keep at 0.005V for 48h, RT, VC free), Sample 8-10 (charge to 0.6V, 1V, 2V, RT, VC free), Sample 11 (discharge to 0.005V and keep at 0.005V for 48h, 55°C, VC free), Sample 12-14 (charge to 0.6V, 1V, 2V, RT, VC free). Sample 15 (discharge to 0.005V and keep at 0.005V for 48h, RT, 2wt. % VC), Sample 16-18 (charge to 0.6V, 1V, 2V, RT, 2wt. % VC).0.005p means potentiostatical discharge at 0.005V for 48h.

3.7 A scheme showing dynamic changed SEI

On the basis of above results and analysis, a scheme of the SEI on silicon anode can be drawn and shown in Figure 12. Initially, the solvents of the electrolyte obtain electron from the anode and be reduced to different kinds of anions or radicals, e.g. CO_3^{2-}, F-, $ROCO_2^{2-}$, et al.. These anions will react with concentrated lithium ions near anode and form lithium salts with different solubility in the electrolyte. The insoluble species will adsorb on the surface of the anode, nucleate and grow into particles, islands to form the first incontinuous layer of the SEI film. The following reduced and formed lithium salts could deposit either on the formed-in-advance SEI islands or naked areas, this is determined by thermodynamic and/or kinetic factors. Homogeneity of the SEI film should be related to the homogeneities of the electrical conductivity of the anode, surface structure of the anode, concentration of electrolyte, electric field distribution near anode and the rate. Therefore, it is not necessary that the SEI film will cover the whole exposed surface of the anode even when the potential of the anode is approaching to the deposition potential of lithium. Accordingly, the thickness of the SEI could exceed electron tunneling length of typical 3nm since the SEI is not dense and not covered the surface completely. Once the solvent can get electrons from the anode, the formation of the SEI during the discharging process cannot be terminated unless the SEI coverage is 100% and no porous structure exists. Because of such competitive processes of reduction, nucleation, growth and dissolution, single layer, double layer and multiple layers could be formed dynamically during discharging, but quite inhomogeneously.

Physical Chemistry Chemical Physics Accepted Manuscript

This journal is © The Royal Society of Chemistry 2012

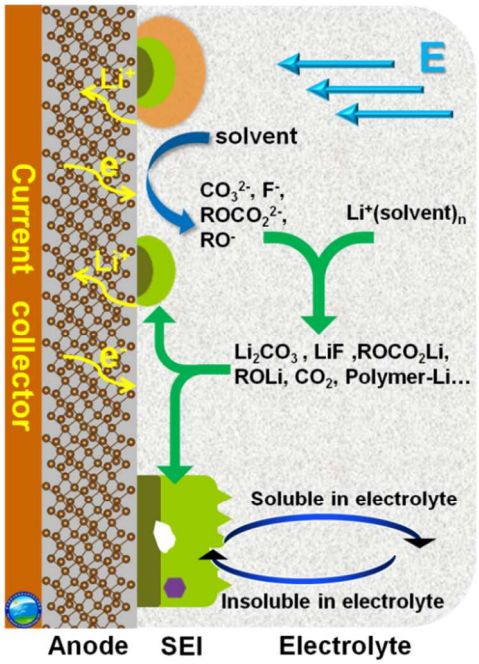

Fig. 12 Dynamic formation scheme of SEI of Anode. The formed SEI can deposit on the surface of electrode, dissolve and drift in the electrolyte.

3.8 Possible developments of the scanning force curve method for detecting SEI films

We have tried to develop *in situ* scanning force curve method to get similar information of the SEI. However, the solvents (i.e. DMC) were evaporated within 10 minutes in the glove box during measuring. The scanning experimental could not be performed. If the solvents are changed into nonvolatile solvents, such as ionic liquid, the information of the SEI on silicon electrode should be very different to commercial available electrolyte. This problem may be solved by improving the scanning rate of SPM technique in future.

As discussed above, we could not extract chemical information simultaneously from the force curve now. This may be improved by measuring Young's modulus of a series of reference thin films on silicon substrate, such as Li_2CO_3, LiF, $ROCO_2Li$, ROLi, PEO-Li. However, it could be difficult for the multi-layer structured or single-layered SEI composed of many components. A better method could be performed by combining tip-enhanced Raman spectroscopy (TERS) during scanning force curve,[32, 33] which also need great effort. We believe that combination of this method with SIMS, XPS, EELS, TG-DSC-MS and ABF-STEM could be helpful to obtain a complete picture of the SEI, including chemical, structure, mechanical properties.

4. Conclusions

In summary, the microstructure and 3D Young's modulus distribution of the SEI on silicon anode can be investigated by *ex situ* force curve method. Main conclusions can be drawn:

1) The SEI on silicon anode is highly inhomogeneous with single, double, mixed-layered, porous structure and sandwiched structure.
2) The thickness of the SEI varies during discharging and charging, from 0-90 nm.
3) Soft SEI parts tend to grow on the outer-layer of the SEI and can be decomposed after charging and increasing temperature.
4) The SEI coverage for fully discharged silicon anode at room temperature is about only 51% and can be improved significantly to 95% after adding 2wt. % VC in the electrolyte.

It is believed that the scanning force curve method (SFCM) used in our research could be extended as a general method to screen and evaluate the electrolyte additive, binder effect, polymer electrolyte in various batteries and other electrochemical devices.

Acknowledgements

Financial support from "Strategic Priority Research Program" of the Chinese Academy of Sciences (Grant No. XDA09010102), National Natural Science Foundation of China for Distinguished Young Scholars (Grant No. 52315206) and National project 973 (Grant No. 2012CB932900) are appreciated.

Notes and references

[a] Beijing National Laboratory for Condensed Matter Physics, Institute of Physics, Chinese Academy of Sciences, Beijing 100190, China
[b] i-Lab, Suzhou Institute of Nano-Tech and Nano-Bionics, Chinese Academy of Sciences, Suzhou, Jiangsu 215123, China

1. J. Tarascon and M. Armand, *Nature*, 2001, **414**, 359.
2. M. Armand and J. M. Tarascon, *Nature*, 2008, **451**, 652-657.
3. J. Tollefson, *Nature*, 2008, **456**, 436-440.
4. J. B. Goodenough and Y. Kim, *Chemistry of Materials*, 2010, **22**, 587-603.
5. H. Li, Z. Wang, L. Chen and X. Huang, *Advanced Materials*, 2009, **21**, 4593-4607.
6. K. Xu, *Chemical Reviews-Columbus*, 2004, **104**, 4303-4418.
7. E. Peled, *Journal of the Electrochemical Society*, 1979, **126**, 2047.
8. H. Li, X. Huang and L. Chen, *Electrochemical and solid-state letters*, 1998, **1**, 241-243.
9. D. Aurbach, K. Gamolsky, B. Markovsky, Y. Gofer, M. Schmidt and U. Heider, *Electrochimica Acta*, 2002, **47**, 1423-1439.
10. M. Inaba, H. Tomiyasu, A. Tasaka, S. K. Jeong and Z. Ogumi, *Langmuir : the ACS journal of surfaces and colloids*, 2004, **20**, 1348-1355.
11. I. T. Lucas, E. Pollak and R. Kostecki, *Electrochemistry Communications*, 2009, **11**, 2157-2160.
12. B. Key, R. Bhattacharyya, M. Morcrette, V. Seznéc, J. M. Tarascon and C. P. Grey, *Journal of the American Chemical Society*, 2009, **131**, 9239-9249.
13. S. Shi, P. Lu, Z. Liu, Y. Qi, L. G. Hector, H. Li and S. J. Harris, *Journal of the American Chemical Society*, 2012, **134**.
14. E. Peled, D. Golodnitsky and G. Ardel, *Journal of the Electrochemical Society*, 1997, **144**, L208-L210.

Physical Chemistry Chemical Physics Accepted Manuscript

15. D. Aurbach, B. Markovsky, M. D. Levi, E. Levi, A. Schechter, M. Moshkovich and Y. Cohen, *Journal of Power Sources*, 1999, **81**, 95-111.
16. M. Winter, *Zeitschrift für Physikalische Chemie*, 2009, **223**, 1395-1406.
17. H. Li, X. Huang, L. Chen, Z. Wu and Y. Liang, *Electrochemical and solid-state letters*, 1999, **2**, 547-549.
18. T. D. Hatchard and J. R. Dahn, *Journal of the Electrochemical Society*, 2004, **151**, A838.
19. C. K. Chan, R. Ruffo, S. S. Hong and Y. Cui, *Journal of Power Sources*, 2009, **189**, 1132-1140.
20. Y. He, X. Yu, G. Li, R. Wang, H. Li, Y. Wang, H. Gao and X. Huang, *Journal of Power Sources*, 2012, **216**, 131-138.
21. J. W. Wang, Y. He, F. F. Fan, X. H. Liu, S. M. Xia, Y. Liu, C. T. Harris, H. Li, J. Y. Huang, S. X. Mao and T. Zhu, *Nano letters*, 2013, **13**, 709-715.
22. Y. H. Wang, Y. He, R. J. Xiao, H. Li, K. E. Aifantis and X. J. Huang, *Journal of Power Sources*, 2012, **202**, 236-245.
23. L. Y. Beaulieu, A. D. Rutenberg and J. R. Dahn, *Microsc Microanal*, 2002, **8**, 422-428.
24. H. Lee, W. Shin, J. W. Choi and J. Y. Park, *J Phys D Appl Phys*, 2012, **45**.
25. L. Martin, H. Martinez, M. Ulldemolins, B. Pecquenard and F. Le Cras, *Solid State Ionics*, 2012, **215**, 36-44.
26. J. Zhang, R. Wang, X. Yang, W. Lu, X. Wu, X. Wang, H. Li and L. Chen, *Nano letters*, 2012, **12**, 2153-2157.
27. V. B. Shenoy, P. Johari and Y. Qi, *Journal of Power Sources*, 2010, **195**, 6825-6830.
28. J. S. Shin, C. H. Han, U. H. Jung, S. I. Lee, H. J. Kim and K. Kim, *Journal of Power Sources*, 2002, **109**, 47-52.
29. J. Domke and M. Radmacher, *Langmuir : the ACS journal of surfaces and colloids*, 1998, **14**, 3320-3325.
30. Y. Zeng, L. Li, H. Li, X. Huang and L. Chen, *Ionics*, 2008, **15**, 91-96.
31. L. B. Chen, K. Wang, X. H. Xie and J. Y. Xie, *Journal of Power Sources*, 2007, **174**, 538-543.
32. Z. Q. Tian, B. Ren, J. F. Li and Z. L. Yang, *Chem Commun*, 2007, 3514-3534.
33. D. Y. Wu, J. F. Li, B. Ren and Z. Q. Tian, *Chem Soc Rev*, 2008, **37**, 1025-1041.

Physical Chemistry Chemical Physics Accepted Manuscript

 This journal is © The Royal Society of Chemistry 2012

Journal Name RSCPublishing

paper

TOC for

3D Visualization of Inhomogeneous Multi-Layered Structure and Young's Modulus of Solid Electrolyte Interphase (SEI) on Silicon Anode for Lithium ion Batteries

Jieyun Zheng,[a] Hao Zheng,[a] Rui Wang,[c] Liubin Ben,[a] Wei Lu,[b] Liwei Chen,[b] Liquan Chen[a] and Hong Li[a*]

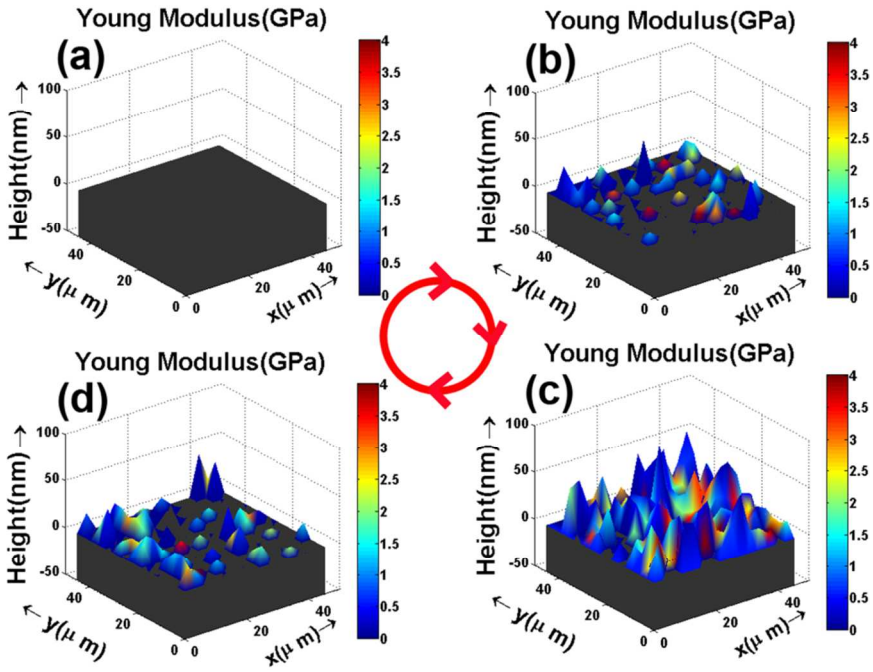

Inhomogeneous multi-layered structure, thickness, Young's modulus and coverage of SEI on silicon anode during cycling are visualized three-dimensionally by scanning force curve method.

Physical Chemistry Chemical Physics Accepted Manuscript